JACS
JOURNAL OF THE AMERICAN CHEMICAL SOCIETY
Article
pubs.acs.org/JACS

# Detecting Substrates Bound to the Secondary Multidrug Efflux Pump EmrE by DNP-Enhanced Solid-State NMR

Yean Sin Ong,[†,§] Andrea Lakatos,[†,§] Johanna Becker-Baldus,[†] Klaas M. Pos,[‡] and Clemens Glaubitz[†,*]

[†]Institute of Biophysical Chemistry & Centre for Biomolecular Magnetic Resonance and [‡]Institute of Biochemistry, Goethe University Frankfurt, Max-von-Laue-Str. 9, 60438 Frankfurt am Main, Germany

Supporting Information

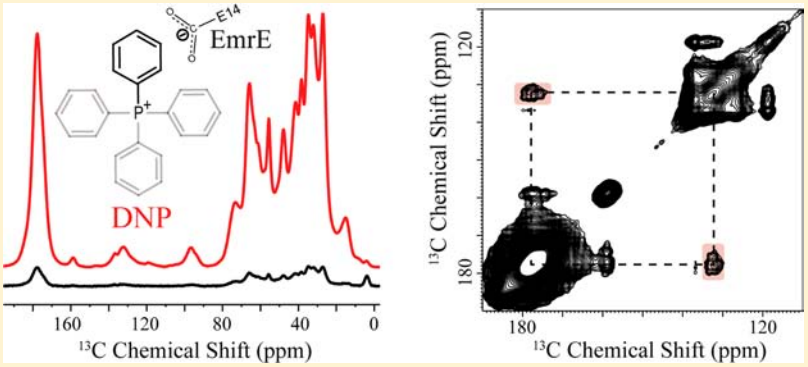


**ABSTRACT:** *Escherichia coli* EmrE, a homodimeric multidrug antiporter, has been suggested to offer a convenient paradigm for secondary transporters due to its small size. It contains four transmembrane helices and forms a functional dimer. We have probed the specific binding of substrates $TPP^+$ and $MTP^+$ to EmrE reconstituted into 1,2-dimyristoyl-*sn*-glycero-3-phosphocholine liposomes by $^{31}$P MAS NMR. Our NMR data show that both substrates occupy the same binding pocket but also indicate some degree of heterogeneity of the bound ligand population, reflecting the promiscuous nature of ligand binding by multidrug efflux pumps. Direct interaction between $^{13}$C-labeled $TPP^+$ and key residues within the EmrE dimer has been probed by through-space $^{13}$C−$^{13}$C correlation spectroscopy. This was made possible by the use of solid-state NMR enhanced by dynamic nuclear polarization (DNP) through which a 19-fold signal enhancement was achieved. Our data provide clear evidence for the long assumed direct interaction between substrates such as $TPP^+$ and the essential residue E14 in transmembrane helix 1. Our work also demonstrates the power of DNP-enhanced solid-state NMR at low temperatures for the study for secondary transporters, which are highly challenging for conventional NMR detection.

## INTRODUCTION

EmrE from *Escherichia coli* is the archetypical member of the small multidrug resistance (SMR) transporter family and one of the smallest (12 kDa) transporters identified so far. It is situated in the inner membrane of the bacteria and exports a wide range of positively charged polyaromatic toxic compounds in exchange for protons.[1−6] Like other SMR proteins, EmrE consists of four transmembrane helices and its minimal functional unit is a homodimer. Due to its small size, stable secondary structure, and preserved activity after purification, EmrE generated great expectations as an ideal model for understanding the functional mechanism of ion-coupled transporters.[7] Based on CryoEM, X-ray, and sequence conservation data, a single-site alternating access model based on an antiparallel dimer with an inward-facing to outward-facing conformational exchange during transport has been proposed.[8] Conformational exchange required for alternating access involves the formation of an occluded state.[9] Further evidence for exchange and structural asymmetry was provided by liquid-state NMR on EmrE in isotropic bicelles.[10] Structural asymmetry is also supported by solid-state NMR on EmrE in magnetically aligned bicelles,[11] consistent with our previous solid-state NMR measurements on E14, the key residue for substrate binding,[2] showing an asymmetric binding pocket.[12] It is interesting to note that multiple topoforms, i.e. both parallel and antiparallel dimers, are functional as shown by genetic and biochemical tools.[7,13]

Biochemical data have clearly shown that the highly conserved E14 in helix 1 seems to coordinate both substrate binding and release and is essential for transport.[2−4,14,15] However, the mechanistic details at the molecular level of this sequential proton−substrate binding and release cycle remain to be solved. Such a central functional role of E14 requires a close proximity between the substrate and E14 side chain, which has not been directly shown yet. The available X-ray structure of EmrE in complex with $TPP^+$, due to its limited resolution (3.8 Å), was only able to show that the E14 residue

**Received:** March 19, 2013
**Published:** September 18, 2013

   dx.doi.org/10.1021/ja402605s | *J. Am. Chem. Soc.* 2013, 135, 15754−15762

points toward the substrate binding chamber.[16] Recent EPR studies gave an insight into the dynamics of EmrE in a site-specific manner, showing that apo-EmrE has a highly flexible conformation. Changes in protein conformation induced by binding of the high-affinity substrate $TPP^+$ have also been characterized.[17]

Here, solid-state NMR is used to provide direct evidence for a close proximity between E14 and the bound substrate in membrane-embedded EmrE. Specific binding, molecular dynamics, and structural heterogeneity within the binding pocket were monitored by $^{31}P$ MAS NMR for the high-affinity substrate tetraphenylphosphonium ($TPP^+$) and its analogue methyltriphenylphosphonium ($MTP^+$).[18] The latter substrate displays an affinity that is reduced by 2 orders of magnitude as compared to $TPP^+$.[18] By synthesizing $TPP^+$ with one of its phenyl rings $^{13}C$-labeled, direct interactions with $^{13}C$-labeled EmrE have been analyzed. Utilizing the considerable sensitivity enhancement provided by dynamic nuclear polarization, we have been able to prove the long assumed direct interaction between the E14 side chain and $TPP^+$. DNP opened the way for studying biological systems that have been inaccessible for solid-state NMR due to low signal intensities. Observation of membrane proteins in their native cellular membranes[19,20] as well as ligands bound to receptors[21] or protein complexes available only at very low quantities[22] became possible. Here, the signal enhancement by DNP and the possibility to perform experiments at low temperatures suppressing unfavorable dynamics of bound $TPP^+$ were essential, which would not have allowed substrate detection under conventional solid-state NMR conditions. The use of low temperatures as well as DNP-enabled signal enhancement, a direct interaction of EmrE E14–side chain and the phenyl ring of $TPP^+$, is proven for the first time and provides insight into the functional mechanism of EmrE.

Due to their intrinsic dynamic properties, secondary transporters have been challenging for structural and spectroscopic studies, but the potential of solid-state NMR was recognized early as demonstrated for the case of sugar transporters,[23] has been explored for EmrE,[11,12,24,25] and is reviewed in refs 26 and 27. Here, we show that enhancing the sensitivity of solid-state NMR by DNP offers promising perspectives for further in-depth studies on secondary transporters.

## RESULTS AND DISCUSSION

**Verifying Substrate Binding Affinity to EmrE Reconstituted into DMPC Bilayers.** It is essential to know whether EmrE exists in a defined oligomeric and functionally relevant state in our proteoliposome preparations for an unambiguous interpretation of spectroscopy data. Cryo-EM[6] and X-ray[16] crystal structures of EmrE show that the basic functional state of EmrE is dimeric. It has been very well established that dimer formation, which takes place in lipids or good membrane mimicking environment, is associated with a high-affinity binding of $TPP^+$. It was found that dimeric EmrE in DDM detergent micelles, bicelles, and lipid bilayers binds $TPP^+$ in the low nanomolar range,[5,10,28–30] while monomeric EmrE in DDM micelles binds $TPP^+$ with much lower affinity in the micromolar range.[31] $TPP^+$ binding can therefore be used to verify formation of functionally correct dimers. In our preparations, a $K_d$ of 1.71 ± 0.35 nM has been found for [$^3$H]-$TPP^+$ bound to EmrE in 1,2-dimyristoyl-*sn*-glycero-3-phosphocholine (DMPC) bilayers (Figure 1), which correlates very well with earlier published data and confirms the formation of a functional dimer. Further binding data are shown in Supporting Information Figure S2.

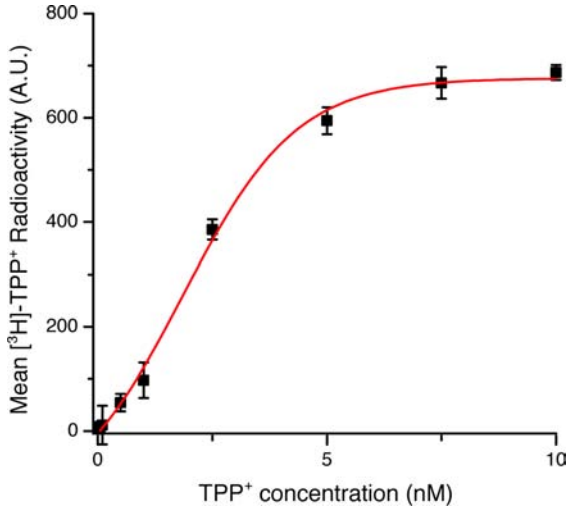


**Figure 1.** Binding of [$^3$H]-$TPP^+$ to EmrE reconstituted into DMPC. Data points are well-described by using a Boltzmann fit with a $K_d$ of 1.7 ± 0.4 nM. The high affinity agrees well with data reported before[2−6] and is a strong indicator for the formation of a functional dimer. The molar lipid to protein ratio was 1:100. Further details are given in the Materials and Methods.

**Identification of Bound Substrates with $^{31}P$ MAS NMR.** Both $TPP^+$ and $MTP^+$, the substrates chosen for this study, contain a phosphorus atom making NMR detection by $^{31}P$ MAS NMR straightforward. $TPP^+$ added to DMPC liposomes without EmrE has a chemical shift of 22.8 ppm, while $MTP^+$ resonates at 21.3 ppm (Figure 2a,b, top row). DMPC has a chemical shift of −1 ppm (not shown). Both substrates could only be detected by $^{31}P$ direct polarization under proton decoupling ($^{31}P$-DP) but not by $^1H$–$^{31}P$ cross-polarization ($^{31}P$-CP), indicating high mobility in the lipid bilayer as reported previously.[24] In contrast, $^{31}P$-CP works well for DMPC liposomes containing EmrE: adding substrate at a molar ratio of EmrE dimer/ligand of 1:2 reveals two signals for $TPP^+$ (22.7 and 22.3 ppm) and $MTP^+$ (21.5 and 19.7 ppm) (Figure 2a,b, middle row). The fact that both substrates can be observed by $^{31}P$-CP indicates that binding to EmrE within the lipid bilayer provides them a more rigid environment compared to DMPC bilayers alone. After washing the proteoliposome samples with buffer, the less shielded signals of both substrates disappear, while the more shielded resonances remain almost unchanged (Figure 2a,b, bottom row). This means that the former signals arise from weakly bound (likely nonspecific) and the latter from a tightly bound (likely specific) substrate population. It can be seen from Figure 2a,b that the remaining $TPP^+$ and $MTP^+$ signals become narrower ($TPP^+$, 62 to 50 Hz; $MTP^+$, 117 to 75 Hz) and are slightly shifted ($TPP^+$, 22.3 to 22.1 ppm; $MTP^+$, 19.7 to 19.3 ppm) after sample washing, which is most likely caused by substrate exchange between the nonspecifically and specifically bound substrate populations.

The assignment of the peak at 22.3 ppm to the specifically bound $TPP^+$ population is also supported by a titration experiment shown in Figure 2c. The peak intensity increases with increasing amounts of substrate but saturates for $TPP^+$/EmrE molar ratios larger than 0.5. This agrees well with data in


dx.doi.org/10.1021/ja402605s | J. Am. Chem. Soc. 2013, 135, 15754−15762

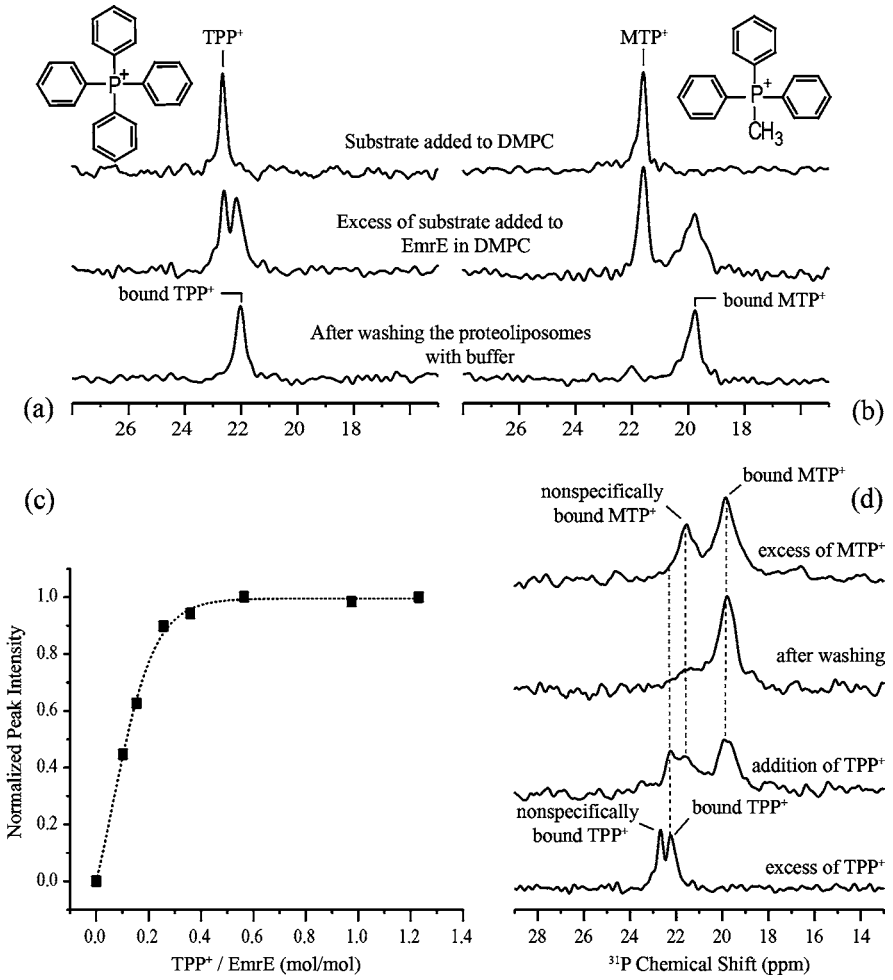


**Figure 2.** Detection of $TPP^+$ (a) and $MTP^+$ (b) specifically bound to EmrE observed by $^{31}P$ MAS NMR. Adding $TPP^+$ and $MTP^+$ to DMPC liposomes results in signals at 22.8 ppm ($TPP^+$) and 21.3 ppm ($MTP^+$) (top row). Adding excess substrate to EmrE reconstituted into DMPC results in two $TPP^+$ populations at 22.3 and 22.7 ppm and two $MTP^+$ peaks at 19.7 and 21.5 ppm (middle row). A molar ratio of two substrates per EmrE dimer was used. The low-field populations show almost identical chemical shifts to those observed in the absence of EmrE and disappear upon sample washing (bottom row). They correspond to free and nonspecifically bound ligands, while the remaining high-field signals result from specifically bound substrates. The latter show slightly smaller chemical shifts ($TPP^+$, 22.1 ppm; $MTP^+$, 19.3 ppm) and more narrow lines. Upon $TPP^+$ titration, the intensity of the signal from the specifically bound population saturates above a molar ratio of 2 EmrE/1 $TPP^+$ (c). Competitive titration experiments show that $TPP^+$ displaces $MTP^+$ bound to EmrE (d). All spectra were acquired using $^1H-^{31}P$ cross-polarization except for $TPP^+/MTP^+$ in pure DMPC bilayers, which were recorded using direct polarization.

Figure 1 and earlier publications showing that the basic functional unit of EmrE is a dimer.[5,6,32] Further addition of $TPP^+$ led to the appearance of the weakly bound $TPP^+$ signal at 22.7 ppm (see Figure S3).

Further evidence for detecting $TPP^+$ specifically bound in the EmrE binding pocket is provided by a competitive titration experiment (Figure 2d). A sample of EmrE reconstituted in DMPC has been loaded with excess $MTP^+$, and nonspecifically bound $MTP^+$ was removed by washing as described above. Upon addition of $TPP^+$, the specifically bound $MTP^+$ signal decreases and the nonspecifically bound population as well as a signal for specifically bound $TPP^+$ appears. These data prove that both the $TPP^+$ signal at 22.3 ppm and the $MTP^+$ signal at 19.3 ppm can be assigned to the specifically bound substrate populations and also show that both ligands occupy the same binding pocket. Furthermore, analyzing CP built-up curves (Figure S4) reveals that both $TPP^+$ and $MTP^+$ have similar dynamics within the substrate binding pocket, which is much reduced compared to nonspecifically bound substrates or lipids as indicated by the steeper signal intensity and faster $T_1\rho_H$ decays (see Supporting Information). This is also supported by comparing $^{31}P$ MAS side band pattern of bound $TPP^+$ and $TPP^+$ in DMPC membranes and in the crystalline form (Figure S5). In liposomes, the $^{31}P$ CSA of $TPP^+$ is completely averaged at this spinning speed indicating fast tumbling. This is consistent with the observation that $TPP^+$ does not cross-polarize in these preparations. The CSA of the crystalline $TPP^+$ is determined to be 20 ppm. $TPP^+$ bound to EmrE has a CSA of 15 ppm, which is approximately 25% lower than that observed in the crystalline form. This lower CSA indicates that, despite the relative immobilization of $TPP^+$ in the EmrE binding pocket, some degree of molecular flexibility still exists.

The spectra in Figure 2a,b show that the $^{31}P$ line width of specifically bound $MTP^+$ ($\Delta\nu_{1/2,MTP^+}$ = 152 Hz) is broader than that of $TPP^+$ ($\Delta\nu_{1/2,TPP^+}$ = 83 Hz). To understand the nature of these differences, we have carried out $^{31}P$ spin–echo experiments to determine $^{31}P$ transverse relaxation times $T_2'$ (Figure S6).[33] For specifically bound $MTP^+$ and $TPP^+$, $T_2'$ values of 4.27 and 6.33 ms were found corresponding to homogeneous line widths of 75 and 50 Hz, which are smaller than the


dx.doi.org/10.1021/ja402605s | J. Am. Chem. Soc. 2013, 135, 15754–15762

experimental line widths, indicating structural heterogeneity in the substrate binding pocket. The large difference between $TPP^+$ and $MTP^+$ is probably caused by a larger heterogeneity of the phosphorus environment in the case of $MTP^+$. The much broader line width of the $MTP^+$ signal is probably due to the fact that the ligand does not have a preferred orientation within the binding pocket of EmrE. The different orientations where the methyl group is experiencing different environments may be reflected in slightly different $^{31}P$ chemical shifts. This orientation dependence is less pronounced for $TPP^+$ where all four substituents are identical and arranged in an almost perfect tetrahedral geometry. Especially the $MTP^+$ data seem to suggest a binding "cavity" instead of a tightly coordinated binding site within the EmrE dimer, in which the substrate/ligand possesses some degree of spatial freedom.

Our data clearly show that specifically bound substrates $TPP^+$ and $MTP^+$ can be detected and that nonspecifically bound populations can be removed, which is of particular importance for direct measurements of substrate−protein interactions as outlined below. In an earlier work, the $^{31}P$ chemical shift of specifically bound $TPP^+$ was found at 19 ppm,[24] which might have been caused by different sample preparation methods. Here EmrE has been solubilized from *E. coli* membranes using the mild detergent DDM as described in the Materials and Methods. In ref 24, the protein was extracted with organic solvents and directly reconstituted in DMPC membranes. It has been later shown that EmrE extracted using organic solvents is mainly monomeric.[34] Therefore, the $TPP^+$ resonance detected at 19 ppm in ref 24 could probably be ascribed to $TPP^+$ bound to monomeric EmrE.

**Detecting $^{13}C$-$TPP^+$ Bound to EmrE by $^{13}C$ MAS NMR.** So far, our $^{31}P$ NMR data show immobilized substrate directly within the binding pocket of EmrE. Direct contact between $TPP^+$ and functionally important residues of $^{13}C$-labeled EmrE could be probed by utilizing, for example, $^{31}P-^{13}C$ dipolar recoupling experiments such as REDOR.[35] However, the $^{31}P$ nucleus of $TPP^+$ is surrounded by four phenyl rings, which prevents close contact to side chain carbons, resulting in relatively weak dipole couplings. Therefore, first $^{31}P-^{13}C$ REDOR experiments resulted in no detectable substrate−protein contact (data not shown). To circumvent this problem, we synthesized $TPP^+$ with one phenyl ring $^{13}C$-labeled ($^{13}C$-$TPP^+$), which would allow detecting protein−ligand interaction directly by $^{13}C-^{13}C$ correlation experiments.

The directly polarized $^{13}C$ MAS spectrum of $^{13}C$-$TPP^+$ in DMPC at 270 K shows three signals appearing as multiplets due to $J$ couplings between the neighboring $^{13}C$ and $^{31}P$ atoms (Figure 3a). Their assignment has been made based on solution NMR data of $^{13}C$-$TPP^+$ (not shown). The $C_{ortho}$ is present as a triplet at 137.2 ppm partly overlapping with the $C_{para}$ at around 137.8 ppm. The $C_{meta}$ appears as a broad peak at 132.7 ppm, and $C_{ipso}$ is detected at 120.3 ppm. Under cross-polarization, $C_{ipso}$ is not observed (Figure 3b). Its cross-polarization efficiency is much reduced since there is no proton directly attached. This observation is consistent with the lack of CP efficiency of the $^{31}P$ nucleus in $TPP^+$ in DMPC liposomes.

Surprisingly, protein-bound $^{13}C$-$TPP^+$ cannot be detected by $^{13}C$−CP MAS NMR at 270 K (Figure 3b), although $^{31}P$-CP MAS NMR on this sample clearly shows specifically bound substrate in complex with EmrE (Figure S7). Therefore, experiments at temperatures from 270 to 103 K have been carried out (Figure 3b). It appears that the $^{13}C$ phenyl ring resonances of EmrE-bound $TPP^+$ are seen only when

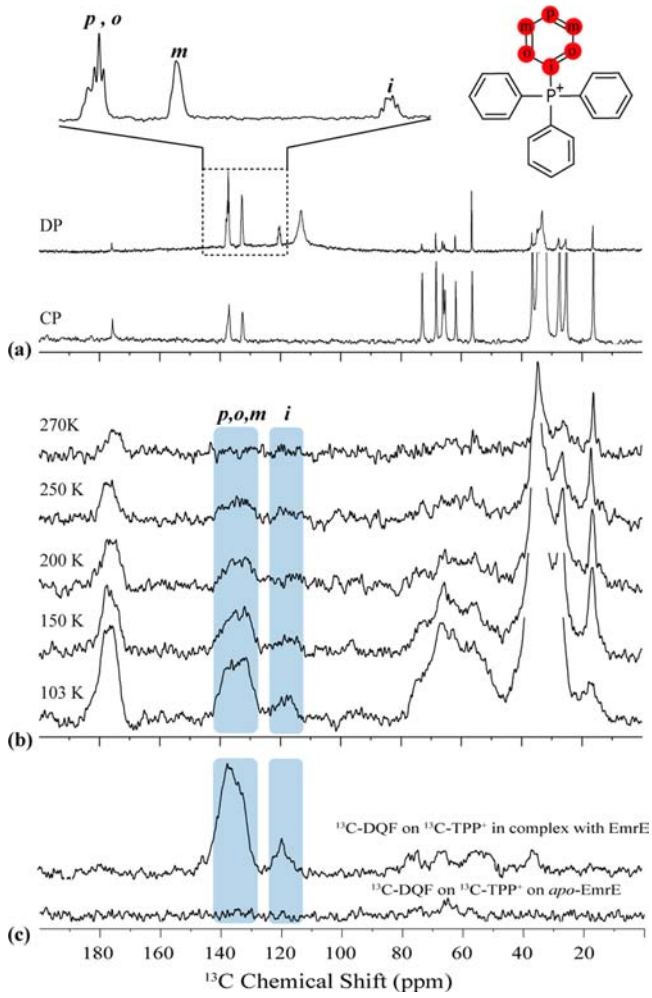


**Figure 3.** Detection of $^{13}C$-labeled $TPP^+$ specifically bound to EmrE observed by $^{13}C$−CP MAS NMR at low temperatures. $TPP^+$ was synthesized with one of its phenyl rings $^{13}C$-labeled and added to DMPC liposomes without EmrE. All $i$ ($C_{ipso}$ at 120.3 ppm), $m$ ($C_{meta}$ at 132.7 ppm), $o$ ($C_{ortho}$ at 137.2 ppm), and $p$ ($C_{para}$ at 137.8 ppm) resonances can be detected by $^{13}C$ direct polarization (DP), while $C_{ipso}$ is not observed using cross-polarization (CP) due to a lack of directly bonded protons (a). Both spectra were acquired at 270 K. $^{13}C$-$TPP^+$ was added to EmrE reconstituted in DMPC. EmrE was not carbon-labeled, and $^{13}C$ is in natural abundance. Nonspecifically bound and free $TPP^+$ populations were removed by one additional washing step. In contrast to the $^{31}P$ CP MAS NMR experiments, bound $TPP^+$ shows only significant CP intensities at temperatures below 200 K, and the phenyl ring resonances are significantly broadened (b). Double-quantum filter (DQF) experiments on the sample from (b) at 103 K confirm that the resonances observed at the highlighted regions originate from $^{13}C$-$TPP^+$ specifically bound to EmrE and not from natural abundance of $^{13}C$ isotopes (c).

temperature is reduced. Unfavorable motions of $TPP^+$ causing line broadening or interfering with CP or decoupling could cause the observed signal loss at higher temperatures. A similar behavior has been reported in the case of the crystalline peptide MLF-OH in which the $^{13}C$ signals of C$\delta$ and C$\varepsilon$ (*ortho* and *meta*) of phenylalanine could not be detected due to phenyl ring flips around the *ipso-para* axis at a rate interfering with the heteronuclear $^1H-^{13}C$ decoupling.[36] The fact that all ring resonances and not only *ortho* and *meta* are missing in our case indicates that besides ring flips also motions of $TPP^+$ itself or of the whole $TPP^+$−protein complex could contribute, as well. On


dx.doi.org/10.1021/ja402605s | J. Am. Chem. Soc. 2013, 135, 15754−15762

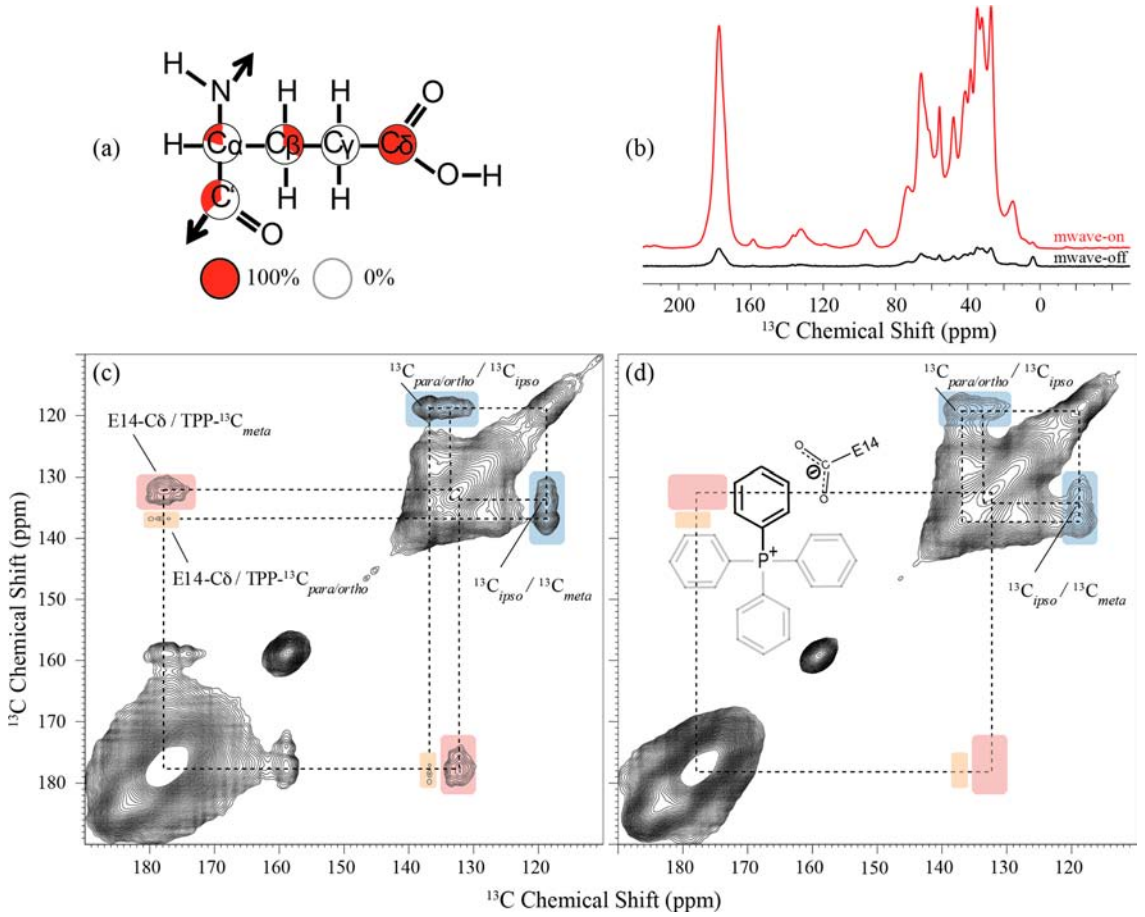


**Figure 4.** DNP-enhanced $^{13}C-^{13}C$ DARR spectrum of $^{13}C$-labeled EmrE in complex with $^{13}C$-TPP$^+$. EmrE was labeled using 2-$^{13}C$-glycerol as sole carbon source, resulting in a sparse isotope distribution in which C$\delta$ of glutamate is 100% $^{13}C$-enriched (a). In these samples, labeling of aromatic amino acids was suppressed to avoid signal overlap with $^{13}C$-TPP$^+$ ($^{13}C$-EmrE$_1$). For DNP, samples were doped with 20 mM TOTAPOL resulting at 100 K in a 19-fold signal enhancement (b). Both spectra were recorded with 32 scans. A $^{13}C-^{13}C$ DARR spectrum (300 ms mixing time) reveals specific through-space correlations between $^{13}C$-EmrE$_1$ and $^{13}C$-TPP$^+$ (c), which are not observed when labeling of glutamates is suppressed ($^{13}C$-EmrE$_2$) (d). The observed correlation therefore arises from a direct interaction between $^{13}C$-TPP$^+$ and the side chain of E14 (see text for further details), and our data indicate a defined orientation of TPP$^+$ with respect to the E14 side chain.

the other hand, our data are consistent with the observation of a correlation between reduced phenyl ring flip rates and increased $^1H-^{13}C$ dipolar couplings with signal intensities when lowering the temperatures below 200 K.[36] Therefore, MAS NMR at low temperatures offers a better dynamic window for detecting $^{13}C$-TPP$^+$ bound to EmrE.

**Probing Direct Interaction between EmrE and TPP$^+$ by DNP-Enhanced $^{13}C-^{13}C$ MAS NMR.** The aim of this study was to prove a direct interaction between TPP$^+$ and E14 in EmrE. Our data show that samples of reconstituted EmrE in complex with specifically bound TPP$^+$ without nonspecifically bound populations can be prepared (Figure 2). TPP$^+$ with one phenyl ring $^{13}C$-labeled ($^{13}C$-TPP$^+$) has been synthesized for detecting through-space contacts to $^{13}C$-labeled EmrE via $^{13}C-^{13}C$ correlation experiments. However, a number of challenges have to be overcome. As shown above, the dynamics of bound $^{13}C$-TPP$^+$ makes detection above 200 K difficult, but working at low temperature provides a solution. Furthermore, due to the symmetry of TPP$^+$ and due to $^{13}C$ labeling of only one of its four phenyl rings, only a certain subpopulation can be expected to show a distinct contact with $^{13}C$-labeled E14 in EmrE. We have therefore utilized dynamic nuclear polarization at low temperature, a novel and highly promising approach to enhance sensitivity of solid-state NMR experiments on membrane proteins.[37]

*Isotope Labeling of EmrE.* It is well-established biochemically that E14 of EmrE is essential for substrate binding.[2−4,14,15] For testing, whether substrates such as TPP$^+$ come in direct contact with this residue, which would provide direct evidence for a direct coordination of proton and substrate binding by E14, its side chain has to be $^{13}C$-labeled. One possibility would be selective glutamate labeling, which is however challenged by isotope scrambling, both *in vivo* and *in vitro*.[38] Instead, we have utilized sparsely $^{13}C$-labeling of EmrE by using 2-$^{13}C$-glycerol as carbon source.[39] This results in a labeling scheme in which the carboxylic carbon C$\delta$ of glutamate is labeled to 100% (Figure 4a). The only three other side chain carbons, which could overlap with the glutamate C$\delta$ signal, are C$\delta$ of glutamine (100% enriched), C$\gamma$ of aspartate (60% enriched), and C$\gamma$ of asparagine (60% enriched).[39] Labeling of aromatic amino acids, which would overlap with $^{13}C$-TPP$^+$ signal in the spectra, was suppressed by supplementing the culture media with unlabeled tyrosine, phenylalanine, tryptophane, and histidine. We refer in the following to this sample as $^{13}C$-EmrE$_1$. As a control, a second sample with the same labeling scheme but additional suppression of glutamate and glutamine labeling was prepared. We refer in the following to this sample as $^{13}C$-EmrE$_2$.


dx.doi.org/10.1021/ja402605s | J. Am. Chem. Soc. 2013, 135, 15754−15762

*Probing Direct Interactions between $^{13}$C-TPP$^+$ and $^{13}$C-Labeled EmrE by DNP-Enhanced $^{13}$C MAS NMR.* $^{13}$C-TPP$^+$ was added to $^{13}$C-EmrE$_1$ reconstituted in DMPC. Specific binding and the absence of nonspecifically bound substrate populations was monitored by $^{31}$P MAS NMR (Figure S7). For DNP, the sample was doped with the polarizing agent TOTAPOL, a highly efficient biradical.[40] Under microwave irradiation, a 20-fold signal enhancement was obtained at 103 K (Figure 4b). Under these conditions, a $^{13}$C−$^{13}$C DARR spectrum was recorded, an experiment monitoring $^{13}$C−$^{13}$C through-space correlations. The spectrum in Figure 4c shows intramolecular cross-peaks within $^{13}$C-TPP$^+$ as well as intermolecular cross-peaks between $^{13}$C-TPP$^+$ and $^{13}$C-EmrE$_1$. The latter includes a larger cross-peak of $^{13}C_{meta}$ (132 ppm/178 ppm) and a smaller cross-peak of $^{13}C_{para}$/$^{13}C_{ortho}$ (136 ppm/178 ppm) with a $^{13}$C resonance of $^{13}$C-EmrE$_1$.

In principle, this correlation could arise from a close proximity of the $^{13}$C-labeled phenyl ring of TPP$^+$ to a glutamate/glutamine C$\delta$ and/or aspartate/asparagine C$\gamma$. The latter possibility can be excluded based on the data shown in Figure 4d, which is the same experiment as in Figure 4c but recorded from $^{13}$C-TPP$^+$ in complex with $^{13}$C-EmrE$_2$. Suppressing labeling of glutamates and glutamines causes a loss of the intermolecular cross-peaks showing that the substrate must be close to one of these amino acids. Apo-state spectra of $^{13}$C-EmrE$_1$ and $^{13}$C-EmrE$_2$ are shown in Figures S8 and S9. The loss of both inter- and intramolecular cross-peaks provides further evidence that indeed substrate−protein and not intraprotein or endogenous lipid−protein interactions are observed.

To exclude the possibility that the observed contact between $^{13}$C-TPP$^+$ and $^{13}$C-EmrE$_1$ arises from a glutamine C$\delta$ or from $^{13}$C carbonyls in the protein backbone, REDOR-filtered experiments have been carried out.[25] In this experiment, all $^{13}$C signals from carbons in close contact to a $^{15}$N nitrogen, such as glutamine C$\delta$ or backbone C′, dephase and are reduced in intensity (Figure S10a). Therefore, corresponding cross-peaks are expected to disappear from a REDOR-filtered $^{13}$C−$^{13}$C DARR spectrum (Figure S10). However, the observed intermolecular TPP$^+$−EmrE contact remains, which prooves that it arises indeed from a glutamate C$\delta$. Our EmrE construct contains the essential E14 in helix 1, E25 in loop 2, and E117 in the C-terminal TEV cleavage site (Figure S11). The last two are not part of the transmembrane domain and not important for binding and transport. We can therefore conclude that the phenyl rings of $^{13}$C-TPP$^+$ within the EmrE binding pocket are found in close spatial proximity to C$\delta$ of the functionally essential residue E14.

The main cross-peak between $^{13}$C-TPP$^+$ and $^{13}$C-EmrE$_1$ reveals a chemical shift of 178 ppm for E14-C$\delta$. This is a value expected for a deprotonated carboxyl carbon and shows that E14 becomes deprotonated upon substrate binding. TPP$^+$ was titrated to reconstituted apo-state samples prepared at pH 8 at which E14 should be protonated due to its unusually high p$K_a$ of 8.5.[29] The chemical shift is within the same range as observed previously for EmrE in complex with ethidium.[12] The heterogeneous line shape of the cross-peaks in the EmrE−substrate complex observed here could be caused by the low-temperature conditions but are also consistent with a certain structural asymmetry.[10,12] Line broadening upon substrate binding in crystalline EmrE preparations has also been reported previously.[25] In the latter study, E14-C$\delta$ has been tentatively assigned in the apo-state to a resonance at 173.3 ppm corresponding to a protonated carboxyl group.

Interestingly, E14-C$\delta$ shows a strong and distinct contact with $^{13}C_{meta}$ of TPP$^+$ at 132 ppm but none with $^{13}C_{ipso}$ and only weak correlations with $^{13}C_{para}$/$^{13}C_{ortho}$. This means that E14-C$\delta$ and $^{13}C_{meta}$ are found within approximately 6 Å from each other, and that the TPP$^+$ phenyl ring assumes a relatively defined orientation within the EmrE binding pocket with respect to the E14 side chain. The distance between the phosphorus nuclei of TPP$^+$ and E14-C$\delta$ must be below approximately 12 Å. However, the widths of both inter- and intramolecular cross-peaks also show a certain degree of heterogeneity within the binding pocket, which agrees with our $^{31}$P MAS NMR data (see above). Furthermore, due to the symmetry of the molecule, each of the four phenyl rings is equally likely to interact with E14, while the noninteracting ring carbons sample different environments in the protein binding pocket. Since only one of the four rings has been labeled, only a subpopulation in which this ring assumes the correct orientations gives rise to the observed cross-peak with E14. This is also seen from the fact that the intramolecular cross-peaks show a broader distribution compared to the intermolecular E14-C$\delta$-$^{13}C_{meta}$ cross-peak.

## SUMMARY AND CONCLUSION

Our $^{31}$P MAS NMR data show that both substrates TPP$^+$ and MTP$^+$ share the same binding site in which they show similarly reduced dynamics. The observed heterogeneity reflects structural plasticity needed for a multidrug efflux pump to recognize a range of substrates, which has also been suggested based on cryo-EM data.[41] The use of $^{31}$P MAS NMR also enabled us to monitor sample conditions under which nonspecifically bound substrate could be removed, a crucial step in order to obtain unambiguous data on direct substrate−protein interaction as described by DNP-enhanced $^{13}$C MAS NMR. This novel method provided the first direct evidence for the long assumed direct contact between TPP$^+$ and E14, which is deprotonated upon substrate binding. The phenyl ring of TPP$^+$ assumes a defined orientation with respect to the E14 side chain (Figure 4d). Although a consensus structure has emerged,[42] our findings are also important due to the lack of real high-resolution X-ray[16] and cryo-EM[6] data, which did not allow direct conclusions about the molecular nature of substrate binding. The close proximity to E14-C$\delta$ in transmembrane helix 1 and the location of both helices opposite to each other within the EmrE dimer means that the vicinity between both helices must be large enough to accommodate a substrate with 10 Å diameter. Our data clearly support a model in which E14 directly coordinates substrate and proton binding and release, but a number of questions remain. It needs to be understood whether both E14 in the EmrE dimer get deprotonated and whether both of them coordinate substrate binding in a symmetric or asymmetric fashion. Here, only contact between TPP$^+$ and deprotonated but not protonated E14 has been observed. This means that either both deprotonated side chains coordinate substrate binding in a similar and simultaneous way or only one E14 is involved while the second one is pointing away from the substrate. Further studies are needed to fully resolve the binding and transport mechanism in detail. Here, we have demonstrated that the use of DNP-enhanced solid-state NMR for such mechanistic studies of secondary transporters, in which not only signal enhancement but also

the temperature induced suppression of motions at unfavorable time scales, offers a promising perspective.

## MATERIALS AND METHODS

**Materials Used.** 2-$^{13}$C-Glycerol was purchased from CortecNet (France) and Sigma-Aldrich. Amino acids (unlabeled) used in the protein expression procedure were purchased from AppliChem Biochemica. 1,2-Dimyristoyl-*sn*-glycero-3-phosphocholine lipids were purchased from Avanti Polar Lipids (Alabaster, Alabama, USA). Radioactive tetraphenylphosphonium bromide, [phenyl-$^{3}$H], was purchased from American Radiolabeled Chemicals. 4-(2-Hydroxy-3-((1-hydroxy-2,2,6,6-tetramethylpiperidin-4-yl)amino)propoxy)-2,2,6,6-tetramethylpiperidin-1-ol (TOTAPOL) was kindly provided by Dr. Jörn Plackmayer, Institute for Physical and Theoretical Chemistry, University of Frankfurt.

**Synthesis of $^{13}$C-Labeled TPP$^+$.** Tetraphenylphosphonium bromide containing one $^{13}$C-labeled phenyl ring was synthesized according to the protocol published by Marcoux and Charette.[43] Briefly, 0.45 mmol (1 equiv) of $^{13}$C-bromobenzene, 141.6 mg (1.2 equiv) of triphenylphosphine, 2.95 mg of $NiBr_2$ catalyst, and 0.15 mL of ethylene glycol were mixed in a 5 mL round-bottom flask. The flask was sealed with a Tefon cap. The reaction mixture was heated at 180 °C in an oil bath for 4 h under continuous stirring. As the reaction proceeded, the solution adopted an intense green color. After 4 h, the flask was cooled to room temperature. The green solution was transferred in a separatory funnel, diluted with dichloromethane (DCM), and washed with 3 × 6 mL water and 6 mL of brine. The organic phase was dried over anhydrous $MgSO_4$, filtered through Celite, and concentrated in a rotary evaporator to ca. 1 mL. Four milliliters of diethyl ether was added under vigorous stirring until a white precipitate formed. The precipitate (TPP$^+$) was filtered through Celite and washed with diethyl ether. The obtained solid material was redisolved in DCM and concentrated to dryness in a rotary evaporator. Then, 106 mg of $^{13}$C-labeled tetraphenylphosphonium bromide was obtained.

**EmrE Expression in *E. coli* Host.** The EmrE construct used in this study has a C-terminal TEV cleavage site followed by a 10× His-tag and was inserted downstream of the IPTG-inducible T7 promoter within the pET16b plasmid via NcoI and XhoI restriction endonuclease sites. The EmrE−His protein was overexpressed in *E. coli* C43 as follows: 50 mL of overnight bacterial preculture (transformed with plasmid pET16b bearing the EmrE construct) in LB media containing 100 μg/mL ampicillin was used to inoculate 1 L of M9 minimal salts media, supplemented with 5 mL of glycerol as carbon source, 2 mM $MgSO_4$, 0.1 mM $CaCl_2$, 10% of vitamin mix solution made from 1 pill of commercial vitamin pill (Centrum), and 100 μg/mL ampicillin. The bacterial culture was allowed to grow at 37 °C to a cell density with absorbance of 0.6 at 600 nm, at which point it was induced with 0.2 mM IPTG. The induced bacterial culture was allowed to grow further at 30 °C for 16−18 h after which the bacterial cells were harvested by centrifugation at 5000*g* at 4 °C. For $^{13}$C-labeling of EmrE, 2-$^{13}$C-glycerol was used as the carbon source. Labeling of all aromatic residues was suppressed by adding 1 mM each of unlabeled tryptophane, histidine, tyrosine, and phenylalanine filtered through a membrane of 0.2 μm pore size to the M9 minimal salts media. We refer to this sample as $^{13}$C-EmrE$_1$. In a second sample, labeling of glutamate and glutamine was suppressed in addition to the aromatic amino acids. This sample is referred to as $^{13}$C-EmrE$_2$.

**Purification and Reconstitution.** To each 10 mg of wet cell pellet harvested at the end of protein expression was added 5 mL of lysis buffer (250 mM sucrose, 150 mM NaCl, 10 mM Tris-Cl pH 7.5, 2.5 mM $MgSO_4$, and DNase I) for cell pellet resuspension. The cell suspension was passed through a cell disruptor (Constant Systems) twice for lysis under a pressure of 1.7 kbar. Undisrupted cells and cellular debris were removed by centrifugation at 6000*g*, 4 °C, after which the membrane fraction was pelleted from the supernatant (collected from the above low-speed centrifugation) using ultracentrifugation at 55 000 rpm (Beckmann rotor Ti70) for 45 min at 4 °C. The membrane extract was homogenized in solubilizing buffer (100 mM NaCl, 50 mM Tris-Cl pH 8.0, 10 mM imidazole, 10% glycerol, and 0.8% (w/v) DDM) and incubated for two nights at 4 °C in this buffer. Unsolubilized membrane extract was removed by ultracentrifugation at 55 000 rpm, and the supernatant was incubated with Ni-NTA resins (Qiagen) for 4 h at 4 °C. Nontarget proteins bound loosely to Ni-NTA were washed off with 10 times the resin column volume of wash buffer (100 mM NaCl, 50 mM Tris-Cl pH 8.0, 10% glycerol, 0.08% (w/v) DDM, 30 mM imidazole). Further washings of the protein-bound Ni-NTA resins were carried out with increasing imidazole concentrations in the wash buffer, up to 50 mM imidazole. EmrE−His was then eluted from the Ni-NTA resins using 300 mM imidazole in the elution buffer (100 mM NaCl, 50 mM Tris-Cl pH 8.0, 0.08% (w/v) DDM). Final EmrE yield of 2.7−3 mg per liter of bacterial culture was obtained.

For reconstitution, a stock DMPC liposome suspension of 4 mg/mL in 20 mM Hepes, 20 mM NaCl, pH 8, was prepared by first dissolving DMPC lipids in approximately 2 mL of chloroform, followed by removal of the organic solvent using a rotary evaporator; buffer was then added to resuspend the dried lipids to give a resultant liposome suspension of 4 mg/mL. To generate homogeneous unilamellar liposomes, the above liposome suspension was passed through a Nucleopore membrane of 0.2 μm pore size (Whatman) within a LIPEX Extruder (LIPEX Biomembranes) three times. The eluted EmrE−His was then added to the target amount of the unilamellar liposome suspension according to the desired protein/DMPC lipid molar ratio. For the sample to be measured by DNP-enhanced NMR, EmrE was reconstituted in a protein/lipid molar ratio of 1:25. For the TPP$^+$ binding assay, EmrE was reconstituted in a protein/lipid molar ratio of 1:100. The protein−lipid mixture was incubated at room temperature for 1 h with constant mixing of the contents, followed by addition of an amount of Biobeads (Biorad) equivalent to 30 times the total mass of DDM detergent present in the volume of protein elution used in the reconstitution reaction. Detergent removal was then carried out for two nights at 4 °C in a glass beaker with constant stirring of the contents using a magnetic stirrer. The resulting proteoliposomes at the end of the reconstitution reaction were removed from the biobeads by passing the suspension through a syringe containing glass fibers.

**Sample Preparation for DNP.** Proteoliposomes were pelleted using ultracentrifugation at 55 000 rpm (Beckman Rotor Ti70) for 30 min at 4 °C. The proteoliposome pellet was resuspended in 1 mL of NMR buffer (20 mM NaCl, 20 mM Hepes, pH 8.0) followed by 3 × 5 min sonications in a water bath (with 1 min incubation on ice at each interval to prevent overheating of the proteoliposomes) to generate homogeneous unilamellar proteoliposomes. $^{13}$C-Labeled TPP$^+$ was added to the proteoliposome resuspension in a molar ratio of 1 TPP$^+$/2 EmrE (final TPP$^+$ concentration was >200 μM). The mixture was incubated at room temperature for 30 min shaking. Excess $^{13}$C-TPP$^+$ in solution and $^{13}$C-TPP$^+$ embedded within the DMPC bilayers were removed by pelleting the proteoliposomes using ultracentrifugation as mentioned above followed by discarding the supernatant and resuspending the proteoliposome pellet in 2 mL of NMR buffer (washing step). Following this, a final proteoliposome pellet to be analyzed by solid-state NMR was obtained by ultracentrifugation at 55 000 rpm for 1 h at 4 °C. Following this, 100 μL of 20 mM Hepes buffer (pH 8.0) containing 20 mM TOTAPOL and 30% glycerol ($H_2O$) was added on top of the proteoliposome pellet and incubated overnight at 4 °C. Prior to the DNP measurement, this buffer was removed and the proteoliposome pellet was then packed into a 3.2 mm rotor. The proteoliposome pellet was then packed into a 3.2 mm rotor. Radioactive binding assays were carried out to verify that the addition of TOTAPOL and glycerol does not influence TPP$^+$ binding (Figure S2).

**Radioactive [$^{3}$H]-TPP$^+$ Binding Assay.** Proteoliposomes containing 0.6 mg of EmrE from the reconstitution reaction described above were pelleted using ultracentrifugation at 55 000 rpm (Beckman Rotor Ti70) for 30 min at 4 °C. The proteoliposome pellet was resuspended in 120 μL of NMR buffer (20 mM NaCl, 20 mM Hepes, pH 8.0), giving a final EmrE concentration of 5 mg/mL. Homogeneous unilamellar proteoliposomes were generated by

sonication for 30 min. [$^3$H]-TPP$^+$ binding assay was performed in a 96-well round-bottom plate (Greiner). One microliter of the proteoliposome suspension was added to 45 $\mu$L of NMR buffer in each well. Various concentrations of [$^3$H]-TPP$^+$ were then added to each well, and the concentrations used ranged from 0.05 to 10 nM. The plate was incubated for 1 h at room temperature. Contents within each well were passed through 96-well plate containing glass filters that were pretreated with 30% PEI for 10 min followed by three washing cycles with 150 $\mu$L of NMR buffer containing 0.1% BSA. Unbound [$^3$H]-TPP$^+$ was washed away by three washing cycles with 150 $\mu$L of NMR buffer containing 0.1% BSA. The filters were dried completely before adding them into 2 mL of scintillation liquid and incubated for 2 h in scintillation vials at room temperature with shaking. At the end of the incubation, [$^3$H] counts were measured. A DMPC liposome control (without EmrE) was done in parallel to obtain a linear relation between [$^3$H]-TPP$^+$ counts against increasing TPP$^+$ concentrations in DMPC liposomes without EmrE. Triplicates of each [$^3$H]-TPP$^+$ concentration tested were carried out. For each data point, [$^3$H] counts from the DMPC liposome control without EmrE (calculated from the linear relation obtained above) were subtracted and all data points were fitted to a Boltzmann function using OriginPro 8.5.1.

**$^{31}$P-CP MAS Experiments.** The $^{31}$P-CP MAS NMR measurements were performed at 159 MHz on a Bruker Avance 400 MHz spectrometer using a 4 mm double-resonance probehead. Five kilohertz magic angle sample spinning speed was applied at a temperature of 280 K. CP was done with $^{31}$P spin-lock field of 83 kHz and a contact time of 2 ms. A proton decoupling field of 83 kHz was applied using the SPINAL64 decoupling sequence. Typically 5−7 mg of EmrE embedded in DMPC liposomes (see above) was used throughout these measurements. The substrates were added to the proteoliposomes prior to packing into the NMR rotor and incubated for 1 h at room temperature. Spectra were recorded at protein to ligand ratios of 1:0.5, 1:1, and 1:1.5. A proper 1:0.5 ratio was achieved by saturating the protein binding site with excess substrate followed by the removal of the substrate excess by washing. For this, samples were taken out from the NMR rotor, resuspended in buffer, and repelleted. Repeating this procedure for a total of three times allows an efficient removal of the substrate excess. Since TPP$^+$ has a nanomolar affinity for EmrE, the dissociation of the protein−ligand complex after removing the excess substrate was negligible. For the titration experiments, TPP$^+$ was added to the proteoliposomes in small steps directly into the NMR rotor. After each addition, the sample was spun in the magnet for 1 h to allow equilibration before recording its $^{31}$P NMR spectrum. For each titration point, 2048 scans were collected.

$^{31}$P $T_2$ and $^{31}$P CSA measurements were performed at 242.9 MHz on a 600 MHz Bruker Avance spectrometer at 270 K. A $^{31}$P spin-lock field of 63 kHz was applied during CP for a contact time of 2 ms. $T_2$ was measured using a simple spin−echo pulse sequence at 10 kHz spinning speed. SPINAL64 was used for proton decoupling with a decoupling power of 71 kHz. The refocusing delay ranged from 0.2 up to 7.4 ms. The sample contained 11.6 mg of EmrE in DMPC liposomes at a protein to lipid molar ratio of 1:25. The protein was first saturated with MTP$^+$, which has a lower affinity to EmrE than TPP$^+$. After washing out the excess of MTP$^+$, the $T_2$ of the specifically bound MTP$^+$ was measured. Then MTP$^+$ was exchanged for TPP$^+$ by resuspending the liposomes in TPP$^+$-containing buffer. The $T_2$ of the specifically bound TPP$^+$ was measured after removing the excess substrate from the sample. For the determination of the CSA of the specifically bound TPP$^+$ signal, $^{31}$P-CP MAS spectra were recorded at 2.2 kHz spinning speed. Fitting of the CSA profile was done by using the line shape fitting/solids tool of Topspin 2.1. Chemical shifts were referenced indirectly to 85% *ortho*-phosphoric acid at 0 ppm via crystalline TEPS (triethylphosphine sulfide) set to 58.4 ppm.

**$^{13}$C MAS NMR and DNP Experiments.** The DNP setup used in this study is as described in ref 22. Essentially, DNP-enhanced solid-state NMR experiments with MAS were carried out at 103 K using a 393 MHz/259 GHz spectrometer equipped with a high-power gyrotron as the microwave source. MAS spinning rates of 8 kHz were used with SPINAL64 decoupling (132 kHz) during signal acquisition. For $^{13}$C cross-polarization, a $^1$H 90° pulse of 1.9 $\mu$s was used, with a contact time of 1000 $\mu$s and recycle delay of 3 s. $^{13}$C−$^{13}$C DARR correlation experiments were carried out using 300 ms of mixing time, with 64 scans and 100 increments. DQF experiments were carried out with the POST-C7 dipolar recoupling scheme with symmetric dipolar excitation and reconversion durations of 125 $\mu$s.[44] Chemical shifts were referenced indirectly via adamantane to DSS. Aquisition and spectra processing were carried out with Topspin 2.1 (Bruker Biospin). $^{13}$C−$^{13}$C DARR correlation spectra were processed using Covariance (Bruker Topspin AU program "covariance").

For the observation of EmrE-bound $^{13}$C-TPP$^+$ using cryo-ssNMR, the DNP setup is used in the absence of the microwave source. Unlabeled EmrE in the same lipid/protein ratio as in the samples used for the DNP measurements is used. A series of 1-D $^{13}$C−CP experiments were carried out at different temperatures of 103, 150, 200, 250, and 270 K. For $^{13}$C cross-polarization, a $^1$H 90° pulse of 1.9 $\mu$s was used, with a contact time of 1000 $\mu$s and recycle delay of 3 s. The number of scans used is 1024. Contact time is found not to affect the S/N in the aromatic region of the spectrum at the higher temperatures of 250 and 270 K, hence the same contact time of 1000 $\mu$s was used at these temperatures.

## ■ ASSOCIATED CONTENT

### Ⓢ Supporting Information

Figure S1: Tricine-SDS PAGE, Western blots. Figure S2: $^3$H-TPP$^+$ saturation binding curves at pH 7.5, 9.1 and in the presence of TOTAPOL and glycerol. Figure S3: $^{31}$P MAS NMR spectra corresponding to Figure 2c. Figure S4: $^{31}$P-CP built-up curves for bound TPP$^+$ and MTP$^+$. Figure S5: $^{31}$P CSA analysis of bound TPP$^+$ from MAS side bands. Figure S6: $^{31}$P MAS spin−echo experiments on bound TPP$^+$ and MTP$^+$. Figure S7: $^{31}$P MAS NMR spectrum of $^{13}$C-TPP$^+$ specifically bound to $^{13}$C-EmrE$_1$. Figure S8: DNP-enhanced $^{13}$C DARR spectra of apo-state $^{13}$C-EmrE$_1$ and $^{13}$C-TPP$^+$ specifically bound to $^{13}$C-EmrE$_1$. Figure S9: DNP-enhanced $^{13}$C DARR spectra of apo-state $^{13}$C-EmrE$_2$ and $^{13}$C-TPP$^+$ specifically bound to $^{13}$C-EmrE$_2$. Figure S10: REDOR-filtered $^{13}$C DARR spectrum $^{13}$C-TPP$^+$ specifically bound to $^{13}$C-EmrE. Figure S11: Topology plot of EmrE. This material is available free of charge via the Internet at http://pubs.acs.org.

## ■ AUTHOR INFORMATION


### Corresponding Author

glaubitz@em.uni-frankfurt.de

### Author Contributions

[§]These authors contributed equally.


### Notes

The authors declare no competing financial interest.

## ■ ACKNOWLEDGMENTS

The work was funded by SFB 807 "Transport and communication across membranes". Y.S.O. acknowledges support by the International Max Planck Research School on Biological Membranes, and A.L. is grateful for initial support by a Marie Curie Intra-European Fellowship (FP7-PEOPLE-2007-2-1-IEF). Lenica Reggie, Vasyl Denysenkov, and Jörn Plackmeyer, Frankfurt, are acknowledged for supporting the DNP experiments. Florian Buhr is acknowledged for initial technical help with $^{13}$C-TPP$^+$ synthesis. We are grateful to Bernd Reif, TU Munich, for his invaluable advice to the experiment in Figure S10.

## ■ REFERENCES

(1) Yerushalmi, H.; Lebendiker, M.; Schuldiner, S. *J. Biol. Chem.* **1995**, *270*, 6856.

(2) Muth, T. R.; Schuldiner, S. *EMBO J.* **2000**, *19*, 234.
(3) Rotem, D.; Salman, N.; Schuldiner, S. *J. Biol. Chem.* **2001**, *276*, 48243.
(4) Steiner-Mordoch, S.; Soskine, M.; Solomon, D.; Rotem, D.; Gold, A.; Yechieli, M.; Adam, Y.; Schuldiner, S. *EMBO J.* **2008**, *27*, 17.
(5) Tate, C. G.; Ubarretxena-Belandia, I.; Baldwin, J. M. *J. Mol. Biol.* **2003**, *332*, 229.
(6) Ubarretxena-Belandia, I.; Tate, C. G. *FEBS Lett.* **2004**, *564*, 234.
(7) Schuldiner, S. *Biochim. Biophys. Acta* **2009**, *1794*, 748.
(8) Fleishman, S. J.; Harrington, S. E.; Enosh, A.; Halperin, D.; Tate, C. G.; Ben-Tal, N. *J. Mol. Biol.* **2006**, *364*, 54.
(9) Basting, D.; Lorch, M.; Lehner, I.; Glaubitz, C. *FASEB J.* **2008**, *22*, 365.
(10) Morrison, E. A.; DeKoster, G. T.; Dutta, S.; Vafabakhsh, R.; Clarkson, M. W.; Bahl, A.; Kern, D.; Ha, T.; Henzler-Wildman, K. A. *Nature* **2012**, *481*, 45.
(11) Gayen, A.; Banigan, J. R.; Traaseth, N. J. *Angew. Chem., Int. Ed.* **2013**, *52*, 10321−10324.
(12) Lehner, I.; Basting, D.; Meyer, B.; Haase, W.; Manolikas, T.; Kaiser, C.; Karas, M.; Glaubitz, C. *J. Biol. Chem.* **2008**, *283*, 3281.
(13) Nasie, I.; Steiner-Mordoch, S.; Gold, A.; Schuldiner, S. *J. Biol. Chem.* **2010**, *285*, 15234.
(14) Rotem, D.; Schuldiner, S. *J. Biol. Chem.* **2004**, *279*, 48787.
(15) Yerushalmi, H.; Mordoch, S.; Schuldiner, S. *J. Biol. Chem.* **2001**, *276*, 12744.
(16) Chen, Y.; Pornillos, O.; Lieu, S.; Ma, C.; Chen, A.; Chang, G. *Proc. Natl. Acad. Sci. U.S.A.* **2007**, *104*, 18999.
(17) Amadi, S. T.; Koteiche, H. A.; Mishra, S.; McHaourab, H. S. *J. Biol. Chem.* **2010**, *285*, 26710.
(18) Adam, Y.; Tayer, N.; Rotem, D.; Schreiber, G.; Schuldiner, S. *Proc. Natl. Acad. Sci. U.S.A.* **2007**, *104*, 17989.
(19) Jacso, T.; Franks, W.; Rose, H.; Fink, U.; Broecker, J.; Keller, S.; Oschkinat, H.; Reif, B. *Angew. Chem.* **2012**, *51*, 432.
(20) Renault, M.; Pawsey, S.; Bos, M. P.; Koers, E. J.; Nand, D.; Tommassen-van Boxtel, R.; Rosay, M.; Tommassen, J.; Maas, W. E.; Baldus, M. *Angew. Chem.* **2012**, *51*, 2998.
(21) Linden, A.; Lange, S.; Franks, W.; Akbey, U.; Specker, E.; van Rossum, B.; Oschkinat, H. *J. Am. Chem. Soc.* **2011**, *133*, 19266.
(22) Reggie, L.; Lopez, J.; Collinson, I.; Glaubitz, C.; Lorch, M. *J. Am. Chem. Soc.* **2011**, *133*, 19084.
(23) Spooner, P. J. R.; Rutherford, N. G.; Watts, A.; Henderson, P. J. F. *Proc. Natl. Acad. Sci. U.S.A.* **1994**, *91*, 3877.
(24) Glaubitz, C.; Groger, A.; Gottschalk, K.; Spooner, P.; Watts, A.; Schuldiner, S.; Kessler, H. *FEBS Lett.* **2000**, *480*, 127.
(25) Agarwal, V.; Fink, U.; Schuldiner, S.; Reif, B. *Biochim. Biophys. Acta* **2007**, *1768*, 3036.
(26) Lakatos, A.; Mors, K.; Glaubitz, C. *Methods Mol. Biol.* **2012**, *914*, 65.
(27) Hellmich, U. A.; Glaubitz, C. *Biol. Chem.* **2009**, *390*, 815.
(28) Miller, D.; Charalambous, K.; Rotem, D.; Schuldiner, S.; Curnow, P.; Booth, P. J. *J. Mol. Biol.* **2009**, *393*, 815.
(29) Soskine, M.; Adam, Y.; Schuldiner, S. *J. Biol. Chem.* **2004**, *279*, 9951.
(30) Yerushalmi, H.; Schuldiner, S. *Biochemistry* **2000**, *39*, 14711.
(31) Sikora, C.; Turner, R. *Biophys. J.* **2005**, *88*, 475.
(32) Butler, P. J.; Ubarretxena-Belandia, I.; Warne, T.; Tate, C. G. *J. Mol. Biol.* **2004**, *340*, 797.
(33) De Paepe, G.; Giraud, N.; Lesage, A.; Hodgkinson, P.; Bockmann, A.; Emsley, L. *J. Am. Chem. Soc.* **2003**, *125*, 13938.
(34) Winstone, T. L.; Jidenko, M.; le Maire, M.; Ebel, C.; Duncalf, K. A.; Turner, R. J. *Biochem. Biophys. Res. Commun.* **2005**, *327*, 437.
(35) Gullion, T.; Schaefer, J. *J. Magn. Reson.* **1989**, *81*, 196.
(36) Bajaj, V.; van der Wel, P.; Griffin, R. *J. Am. Chem. Soc.* **2009**, *131*, 118.
(37) Maly, T.; Debelouchina, G. T.; Bajaj, V. S.; Hu, K. N.; Joo, C. G.; Mak-Jurkauskas, M. L.; Sirigiri, J. R.; van der Wel, P. C. A.; Herzfeld, J.; Temkin, R. J.; Griffin, R. G. *J. Chem. Phys.* **2008**, *128*, 052211.
(38) Fujiwara, K.; Nomura, S. M. *PLoS One* **2013**, *8*, e54155.
(39) Castellani, F.; van Rossum, B.; Diehl, A.; Schubert, M.; Rehbein, K.; Oschkinat, H. *Nature* **2002**, *420*, 98.
(40) Song, C. S.; Hu, K. N.; Joo, C. G.; Swager, T. M.; Griffin, R. G. *J. Am. Chem. Soc.* **2006**, *128*, 11385.
(41) Korkhov, V. M.; Tate, C. G. *J. Mol. Biol.* **2008**, *377*, 1094.
(42) Korkhov, V. M.; Tate, C. G. *Acta Crystallogr., Sect. D* **2009**, *65*, 186.
(43) Marcoux, D.; Charette, A. B. *Adv. Synth. Catal.* **2008**, *350*, 2967.
(44) Hohwy, M.; Jakobsen, H. J.; Eden, M.; Levitt, M. H.; Nielsen, N. C. *J. Chem. Phys.* **1998**, *108*, 2686.